ChemPubSoc Europe

DOI: 10.1002/chem.201500105

CHEMISTRY A European Journal Full Paper

Dynamic Covalent Reactions

Dynamic Aminal-Based TPA Ligands**

Yuntao Zhou,[a, b] Yaofeng Yuan,[b] Lei You,*[a] and Eric V. Anslyn*[c]

Abstract: The use of dynamic covalent reactions (DCRs) is gaining popularity for the construction of self-assembling architectures. We have recently introduced DCRs that exchange alcohols and aldehydes to create hemiaminal ethers within tri(2-picolyl)amine (TPA) ligands, all of which are templated by Zn^{II}. To expand the scope of this assembly, aromatic imines derived from pyridine-2-carboxyaldehyde were explored as dynamic covalent receptors for di(2-picolyl)amine in the presence of Zn^{II} to create TPA ligands that contain aminal linkages. This represents another metal-templated in situ multicomponent assembly. The stability of the assembly was successfully modulated through substituent effects, and the equilibrium constants from imines to aminals were correlated by a linear free energy relationship (LFER) with σ^+ values. Dynamic component exchange was investigated as a means of probing multiple equilibriums quantitatively in the system. Further, the mechanism was analyzed with a qualitative kinetics study. NMR spectra reveal the different extents of two competing pathways for assembly depending upon whether the aromatic amine has electron-withdrawing or electron-donating groups on the ring. Finally, mass spectral evidence supports the presence and differing extents of dominance of the two pathways as a function of the substituents.

Introduction

The field of dynamic covalent chemistry (DCC) has been burgeoning in the past decade,[1] with the ultimate goal of building dynamic combinatorial libraries,[2] constructing molecular assemblies and nanomaterials,[3] and modulating biological structures and functions.[4] Reversible covalent bonding can lead to dynamic component exchange as does its noncovalent counterpart, and dynamic covalent reactions (DCRs) lead to in situ-generated molecular diversity and complexity with a much higher efficiency than traditional stepwise covalent synthesis. In spite of the increasing popularity in chemical and biological applications, the chemical space for current DCRs is rather limited. The most used DCRs are imine condensation and exchange,[5] hydrazone condensation and exchange,[6] disulfide exchange,[7] and cyclic boronate ester formation.[8] Both the thermodynamic and kinetic properties often need to be optimized for the development of DCRs for specific purposes.[9]

The chemistry of carbonyl compounds is highly diverse, encompassing condensations, alkylations, cyclizations, and so on, and hence provides an excellent platform for the discovery of new DCRs. Indeed, the aforementioned imine and hydrazone DCRs are based on carbonyl reactivity, and are in part thermodynamically driven by the loss of a water molecule. In contrast to condensation with primary amines, the addition reactions of aldehydes/ketones with alcohols, thiols, and secondary amines are more sluggish and not as thermodynamically favored, and therefore, the formation of organic heterocycles[10] or metal-templated macrocycles[11] are commonly used to stabilize the products: Hemiacetals/acetals, hemithioacetals/thioacetals, and hemiaminals/aminals, respectively.

Recently, we reported a strategy of stabilizing hemiaminal ethers for a broad range of secondary alcohols using in situ-generated tri(2-picolyl)amine (TPA)-like metal complexes (Scheme 1 a).[12] The thermodynamic driving force resulting from metal coordination shifts the equilibrium toward the desired product, which is otherwise unfavorable. Herein, we describe that this four-component assembly that incorporates alcohols creating hemiaminal ethers can be expanded to incorporate aromatic amines, thereby yielding aminals. The experiments reveal the dependence of the assembly equilibrium and mechanism on changes in substituents, as well as the ability to exchange components of multiple equilibria in the assembly mixture, further expanding the scope of DCRs.

[a] Y. Zhou, Prof. Dr. L. You
State Key Laboratory of Structural Chemistry
Fujian Institute of Research on the Structure of Matter
Chinese Academy of Sciences
Fuzhou, 350002 (P.R. China)
E-mail: lyou@fjirsm.ac.cn

[b] Y. Zhou, Prof. Dr. Y. Yuan
College of Chemistry, Fuzhou University
Fuzhou, 350116 (P.R. China)

[c] Prof. Dr. E. V. Anslyn
Department of Chemistry
The University of Texas at Austin
Austin, Texas, 78712 (USA)
E-mail: anslyn@austin.utexas.edu

[**] TPA = Tri(2-picolyl)amine.

Supporting information for this article is available on the WWW under http://dx.doi.org/10.1002/chem.201500105.

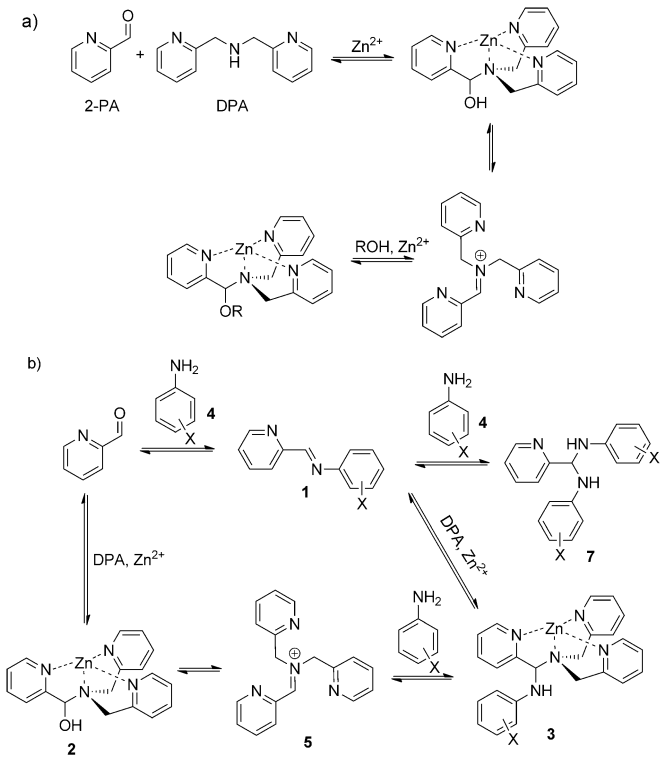

Scheme 1. a) The multicomponent assembly with alcohols; b) The possible pathways for multicomponent assembly with primary aromatic amines.

Results and Discussion

Design of a model system

The reaction of pyridine-2-carboxaldehyde (2-PA), di(2-picolyl)-amine (DPA), zinc triflate, and an alcohol, creates hemiaminal ether complexes in the presence of a Brønsted acid (Scheme 1 a).[12b] We envisioned that analogous assemblies could be performed by using primary aromatic amines (**4**), or potentially from isolated imines. In contrast to the alcohol assembly, in which the reaction proceeds through a tris(pyridine)-substituted iminium ion **5**, we reasoned that the use of aromatic amines would proceed primarily through imine intermediates due to the higher nucleophilicity of **4** relative to secondary alcohols. Thus, in Scheme 1 b the prediction was that the pathway from **4** and 2-PA to **3** would be dominated by imines (**1**) rather than the iminium. Moreover, such an in situ assembly of 2-PA and **4** would minimize the synthetic efforts by avoiding the isolation of the imine, but would afford similar equilibrium mixtures because the reaction is under thermodynamic control.

Reaction screening

To test our hypothesis, we screened the reaction of 2-PA, DPA, and 4-methylaniline under a variety of conditions. The reactions were stirred with 3 Å molecular sieves in deuterated acetonitrile at room temperature overnight and studied by ^{1}H NMR spectroscopy. As expected, the aldehyde peak at $\delta =$ 10 ppm completely disappeared, and only imine **1** was detected if no Zn^{2+} was present (see the Supporting Information), in agreement with our previous results demonstrating that the metal ion is crucial to shift the equilibrium toward the hemiaminal **2**.[12a] However, there were no corresponding peaks of complex **2** or **3** even with the presence of Zn^{2+} in the mixture, although all aldehyde converted to imine **1**. We reasoned that there is not enough driving force to offset the relative inertness of imine **1** under these conditions.

The lack of a coordinating counterion to the Zn^{II} in **3** means that the complex must form solely with a solvent occupying the open site on zinc. This paves the way for manipulating the equilibrium using exogenous ligands. The assembly reaction was hence conducted with 1 equivalent of tetrabutylammonium chloride. After 24 h, no further changes in the ^{1}H NMR spectra were observed, and a similar pattern of resonances as the tripodal TPA complexes when using alcohols were present. The appearance of two sets of doublets at $\delta = 5.55$ and 5.70 ppm (H_a and H_b, $J = 12$ Hz), as well as four sets of doublets between $\delta = 3.75$ and 4.50 ppm (H_d, $J = 16$ Hz, germinal coupling: one at $\delta = 4.45$ ppm; one at 4.25 ppm; the other two around $\delta = 4.00$ ppm overlapped with other peaks), indicates the formation of complex **3**, in which a new stereocenter makes the four methylene protons diastereotopic (Figure 1).

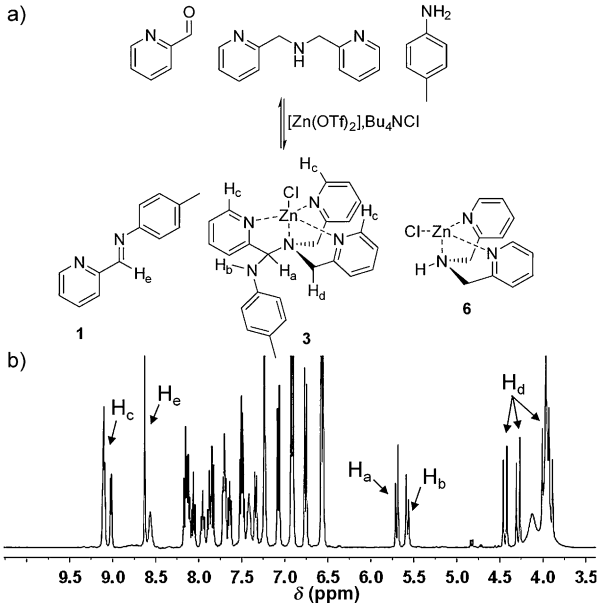

Figure 1. a) The dynamic covalent assembly and b) its ^{1}H NMR spectrum. The resonances of methylene protons in DPA-Zn^{II} (**6**) are between $\delta = 3.75$ and 4.25 ppm and overlap with another two peaks of benzylic protons (H_d) in **3**.

The resonances of methine ($\delta = 5.70$ ppm, H_a) and NH proton ($\delta = 5.55$ ppm, H_b) were further assigned by proton exchange after the addition of D_2O. The aromatic portion of the spectrum reveals the existence of imine **1**, as well as the DPA-Zn^{II} complex (**6**), and hence these components are in equilibrium with **3**. The ratio of **1** and **3** is 1.35, reflecting a yield of 43 %. The formation of **3** was further validated by its corresponding *m/z* peak of 494.4 [**3** + Cl] in the ESI mass spectrum (the Sup-

porting Information, Figure S17). Br^-, I^-, and OAc^- counterions also increase the formation of **3**, but to a lesser extent than Cl^-. The enhancement effect of counteranions is likely due to stabilization of zinc complex through ligand coordination in the axial position.[12]

Equilibrium constants

Having confirmed the formation of **3** by a multicomponent assembly reaction, the next step was to measure the equilibrium constants. Because multiple equilibria exist in the solution, we set out to simplify the system. First, none or only a residue of 2-PA was detected after the equilibrium was reached. Second, although imine **1** and the remaining DPA can both coordinate zinc,[13] the assumption was made that the non-reactive zinc is predominately bound to DPA to form complex **6**. Thus, we chose the following reaction to derive the equilibrium constants [Eq. 1], as this two-component system will directly correlate with the reactivity of imine **1**. All concentrations in Equation (1) can be deduced from the ^{1}H NMR integrals, as well as the mass balance of 2-PA and zinc. By defining the integral ratio of **1** to **3** as *x*, and the total integral of other possible products from 2-PA (i.e., **2** and **7**, see Scheme 1 b) to **3** as *y* (for 4-methylaniline, $y \approx 0$), the specific expression of *K* as given in Equation (2) can be derived (see the details in the Supporting Information).

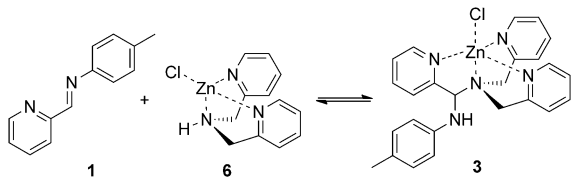

1 6 3

$$K = [\mathbf{3}]/\{[\mathbf{1}][\mathbf{6}]\} \quad (1)$$

$$K = (1 + x + y)/\{x(x + y)[\text{2-PA}]_{\text{total}}\} \quad (x = [\mathbf{1}]/[\mathbf{3}],\ y = ([\mathbf{2}] + [\mathbf{7}])/[\mathbf{3}]) \quad (2)$$

For 4-methylaniline, the apparent equilibrium constant was determined to be 25 M^{-1}, a value much smaller than the assembly of 2-PA and DPA-Zn^{II} to create **2** (*K* around 6600 M^{-1}).[12a] This is in agreement with the higher stability of an imine (starting point for assembly to **3** in [Eq. 1]) than its parent aldehyde (starting point for the alcohol assembly, Scheme 1 a). Nevertheless, the equilibrium does reveal the potential of aromatic imines for the development of new DCRs.

LFER-based modulation

The next goal was to increase the stability of the assembly by varying the electronic nature of the building blocks. It is well known that functional groups on the aromatic rings significantly affect their reactivity in electrophilic substitution reactions, with electron-donating and electron-withdrawing group activating and deactivating the ring, respectively. We postulated that the reactivity of imine **1** could be similarly fine-tuned by the substituent on the aromatic amine due to conjugation of the benzene ring and the C=N functional group.[14] The physical organic tool of choice to study this would be the Hammett linear free energy relationship (LEFR), which quantifies substituent electronic effects.[15] This LFER has been extensively employed to correlate kinetic and thermodynamic data to elucidate associated mechanisms.[16] However, the utilization of Hammett equation for the development of new DCRs has been rarely reported.

A series of aromatic amines with *para* or *meta* substituents, including -OCH_3, -CH_3, -F, -Br, -CF_3, -CN, and -NO_2, were used in the assembly reaction with 2-PA, DPA, zinc triflate, and tetrabutylammonium chloride. The mixture was allowed to stir for 24 h, and the equilibrium constant was determined as described above. The *x*, *y*, *z*, and *K* values are listed in Table S1 (the Supporting Information). In all cases, the corresponding imine **1** and complex **3** are present at equilibrium, but to differing extents. Generally, electron-withdrawing groups facilitate the formation of **3**, whereas electron-donating groups favor imine **1**. 4-Nitroaniline afforded the largest *K* value (304 M^{-1}), whereas *p*-methoxy gave the worst ($K = 8.4$ M^{-1}).

With all equilibrium constants in hand, they were then subjected to a Hammett analysis. An attempt to correlate log *K* with σ did not give a linear relationship, with *p*-OCH_3 significantly deviating from the line (the Supporting Information, Figure S4), indicative of different stabilizing or activating mechanism. To quantify the resonance effect and separate it from the inductive effect, σ^+ values were employed. This parameter accounts for resonance effects as a consequence of direct resonance between the reaction site and the *para* electron-donating or electron-withdrawing group, respectively.[15b] Since these interactions are impossible when the substituent is attached to the *meta* position, the original σ values of *meta* substituents are still valid. A plot of log *K* versus σ^+ indeed afforded a linear line (Figure 2, $r^2 = 0.981$). The substituent *p*-F can be modestly electron-donating ($\sigma^+ = -0.07$), and this is confirmed by the *K* values for 4-fluoroaniline and aniline derived assembly, respectively (43 and 65 M^{-1}).

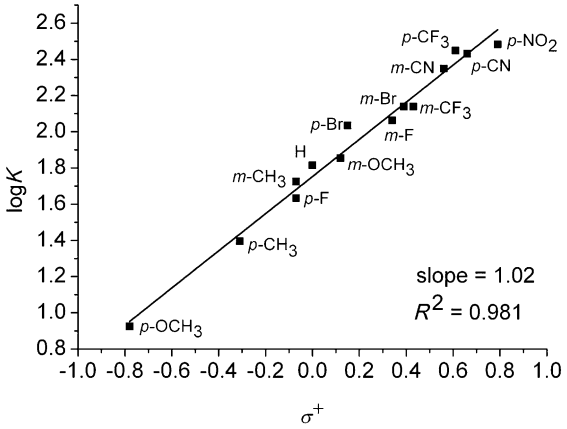

Figure 2. Hammett plot for the reaction of imine **1** with DPA-Zn^{II}.

The linear correlation of log K with σ^+ was rationalized by using resonance structures (Scheme 2). Because an equilibrium exists between imine **1** and assembly **3**, resonance effects on either of these species will be reflected in the Hammett plot.

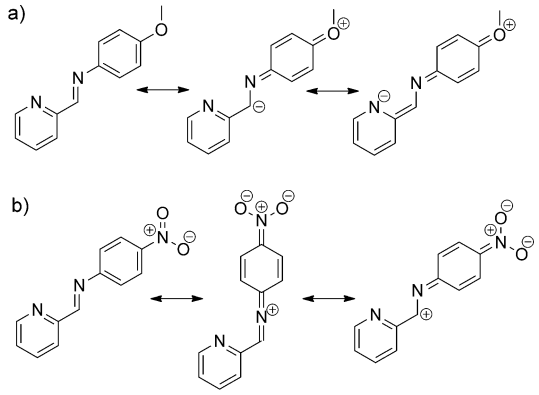

Scheme 2. Resonance structures of aromatic imines with a) p-OCH_3 and b) p-NO_2.

There is no resonance interaction between the substituents and the aminal center of **3**, but instead only induction would be relevant. However, as with the quinoidal resonance interactions in benzylic carbocations and phenoxides, resonance structures can be drawn for imine **1**. p-OCH_3 donates a pair of electrons to the electron-deficient pyridine to stabilize imine **1** (Scheme 2a). Moreover, the partial negative charge on the imine carbon from a contributing structure explains the relative inertness of **1** (i.e., less of complex **3**). In contrast, for the electron-withdrawing nitro group, a quinoidal resonance interaction leads to an imine that is more electrophilic (Scheme 2b). The high reactivity of **1**(p-NO_2) is further supported by a small amount of aminal **7** in the reaction mixture. In another way of considering the data, because the resonance is in the reactant, the σ^+ value is appropriate for correlating the dissociation of complex **3** into imine **1** and **6** with a negative ρ value because the reactant imine carbon is partially positively charged. The reverse reaction (the reaction of **1** and **6** to create **3**) would thereby have a positive ρ value, as we observed.

Dynamic component exchange

Having modulated the DCRs through LFER analysis, component exchange was conducted to verify the reversibility of the assembly system. The reaction was first conducted with 3 equivalents of 4-methylaniline, followed by the addition of equal equivalents of 4-methoxyaniline. The equilibrium was reached after 24 h, and ^{1}H NMR spectroscopy revealed a decrease of 4-methylaniline-derived complex **3** with a concomitant increase in the analogous assembly incorporating 4-methoxyaniline (Figure 3). Upon the reversal of the sequence of addition of amines, the same distribution of components was observed. Moreover, the competition experiments afforded the same results as the component exchange, thereby further confirming the reversibility of the multicomponent assembly.

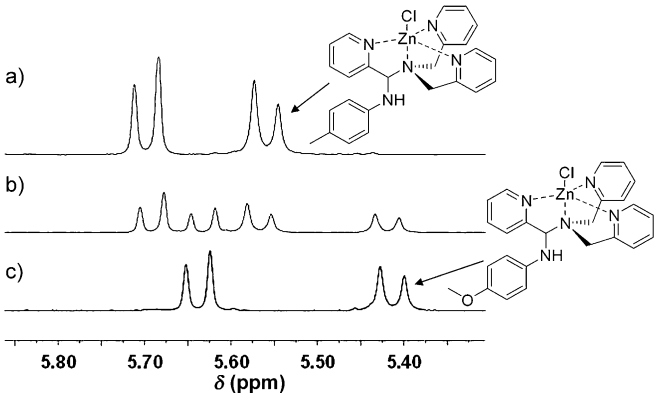

Figure 3. ^{1}H NMR spectra of dynamic covalent assembly derived from a) 4-methylaniline and c) 4-methoxyaniline and b) their component exchange.

Analogous component exchange was also conducted with p-Br and p-CF_3-substituted amines (the Supporting Information, Figures S8 and S9).

To study the associated dynamic covalent bonding within the multicomponent assembly quantitatively, equilibrium constants of a series of dynamic component exchanges were calculated. Because imine **1**, tripodal complex **3**, as well as their corresponding aromatic amines were present in the equilibrium mixture, imine/amine exchange [Eq. (3)], aminal/amine exchange [Eq. (4)], and imine/aminal exchange [Eq. (5)] were investigated (Table 1). For example, the equilibrium constant

Table 1. Equilibrium constants of exchange reactions.

X	K_1	K_2	K_3[a]	K_3[b]
p-OCH_3	3.47	1.01	0.289	0.339
p-CH_3	1.00	1.00	1.00	1.00
p-Br	0.132	0.349	2.65	4.36
p-CF_3	0.021	0.181	8.59	11.3

[a] Derived from exchange reactions [Eq. (5)] and used for LFER analysis. [b] Calculated from Equation (6).

(K_1) for the reaction of **1**(p-CH_3) with p-methoxyaniline is 3.47, therefore favoring **1**(p-OCH_3). The K_1 values for other amines are listed in Table 1, and their trend (p-$OCH_3 > p$-$CH_3 > p$-F $> p$-CF_3) is consistent with the nucleophilicity of the amine and hence its reactivity toward 2-PA. Moreover, a linear relationship was afforded when the value of log K_1 was plotted against σ^+ (slope $= -1.63$, $r^2 = 0.985$, see Figure 4). The negative ρ value is due to stabilization of the product imine through a resonance effect by electron-donating groups.

For the exchange of amines within aminal complex **3**, there is a decrease in equilibrium constant (K_2) as the amine becomes less nucleophilic (p-$OCH_3 \approx p$-$CH_3 > p$-F $> p$-CF_3) as may be expected. However, the difference between electron-rich and electron-deficient amines on K_2 (for example, K_2(p-OCH_3)/K_2(p-CF_3) = 5.58) is significantly smaller than that for imine/amine exchange (in comparison, K_1(p-OCH_3)/K_1(p-CF_3) = 165). The influence of the nucleophilic character of the amine should indeed be far less in complex **3** than in **1** because one

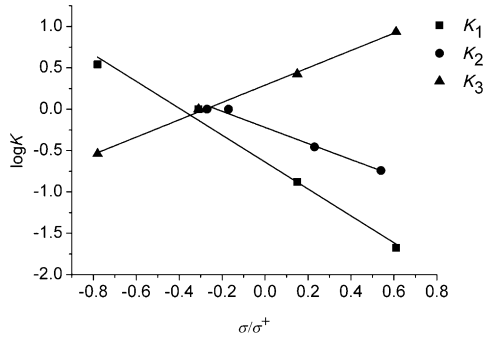

Figure 4. Hammett plot for imine/amine exchange (log K_1 vs. σ^+), aminal/amine exchange (log K_2 vs. σ), and imine/aminal exchange (log K_3 vs. σ^+).

would expect the sigma bond strengths in **3** to be less affected by the identity of the amine than the combination of sigma and pi bonds in **1**. A second rationalization comes from the thermodynamic driving force of zinc coordination, which minimizes the impact of the amines.[17] Because only inductive effects exist between substituents X and the aminal center of **3**, log K_2 was plotted against the standard Hammett parameter σ, and a linear line was obtained ($r^2 = 0.981$, Figure 4). The lower sensitivity toward substitution for aminal/amine exchange than imine/amine exchange was also supported by the smaller absolute value of the slope ρ (-0.972).

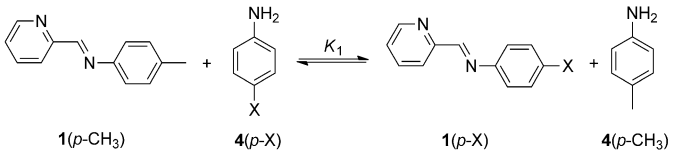

$$K_1 = [\mathbf{1}(p\text{-X})][\mathbf{4}(p\text{-CH}_3)]/\{[\mathbf{1}(p\text{-CH}_3)][\mathbf{4}(p\text{-X})]\} \quad (3)$$

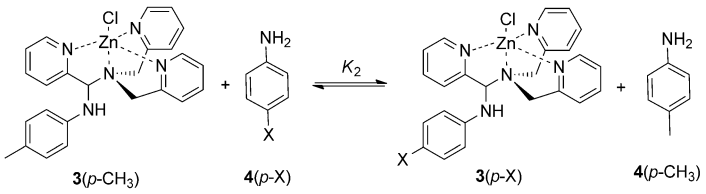

$$K_2 = [\mathbf{3}(p\text{-X})][\mathbf{4}(p\text{-CH}_3)]/\{[\mathbf{3}(p\text{-CH}_3)][\mathbf{4}(p\text{-X})]\} \quad (4)$$

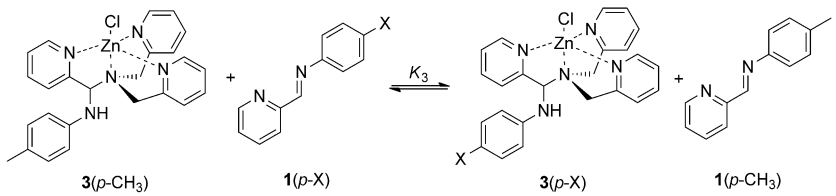

$$K_3 = [\mathbf{3}(p\text{-X})][\mathbf{1}(p\text{-CH}_3)]/\{[\mathbf{3}(p\text{-CH}_3)][\mathbf{1}(p\text{-X})]\} = K_2/K_1 \quad (5)$$

$$K_3 = [K(p\text{-X})]/[K(p\text{-CH}_3)] \quad (6)$$

Due to the differential response of K_1 and K_2 toward substitution, the value of K_3 increases as the arene becomes more electron-deficient (p-$OCH_3 < p$-$CH_3 < p$-F $< p$-CF_3). It is notable that the equilibrium constant obtained from exchange reactions is comparable to that calculated from Equations (2) and (6), considering that several approximations were made to derive Equation (2). Analogous to the K value, the plot of log K_3 versus σ^+ is linear ($R^2 = 0.998$, Figure 4) with a positive ρ value (1.05).

Mechanism studies

We next set out to further distinguish the two possible mechanistic pathways given in Scheme 1b. Although DCRs are thermodynamically controlled, the elucidation of mechanism is beneficial for future design as well as optimization of reaction rates that are crucial to the practicality of DCRs. Qualitative kinetics experiments were performed to determine relative rates, and to potentially spectroscopically observe the intermediates and their transformations. The assembly reactions were run with p-OCH_3, m-F, and p-NO_2-substituted amines in the absence and presence of 1 equiv of pyridinium triflate, and ^{1}H NMR spectra were recorded after 1.5, 5, and 24 h, respectively. These three aromatic amines were chosen to cover a broad range of σ^+ values. The Brønsted acid was utilized as a means of catalyzing the assembly as well as modulating the reaction pathway. For electron-donating p-OCH_3, the equilibrium was reached after 1.5 h with or without acid (the Supporting Information, Figures S10 and S11). Both imine **1** and complex **3** were observed, but no other intermediates were apparent. These results indicate the domination of the imine pathway, which is in agreement with the high nucleophilicity of 4-methoxyamine.

For the 3-fluoroaniline assembly without acid, the hemiaminal **2** was present after 1.5 and 5 h (Figure 5b). But after 24 h, only a trace amount of **2** was detected, suggesting that **2** gradually transforms to complex **3** (the Supporting Information, Figure S12). In the presence of the acid, hemiaminal **2** was in the mixture after 1.5 h, but to a lesser extent (Figure 5c). After 5 h, equilibrium was reached and no hemiaminal **2** was observed (the Supporting Information, Figure S13). We rationalize these observations as acceleration of both pathways through acid catalysis, although the imine mechanism still outweighs the competing iminium route.

When using the highly electron-withdrawing p-NO_2 group on the aromatic amine, aminal **3** was the major component after 1.5 h, although significant amounts of 2-PA and complex **2** existed (Figure 5d). However, at this time period the percentage of imine **1** was much smaller than with p-OCH_3 and m-F-substituted amines. When the reaction was conducted for a longer period (i.e., 5 and 24 h), the corresponding peaks of 2-PA as well as hemiaminal **2** decreased while the amount of assembly

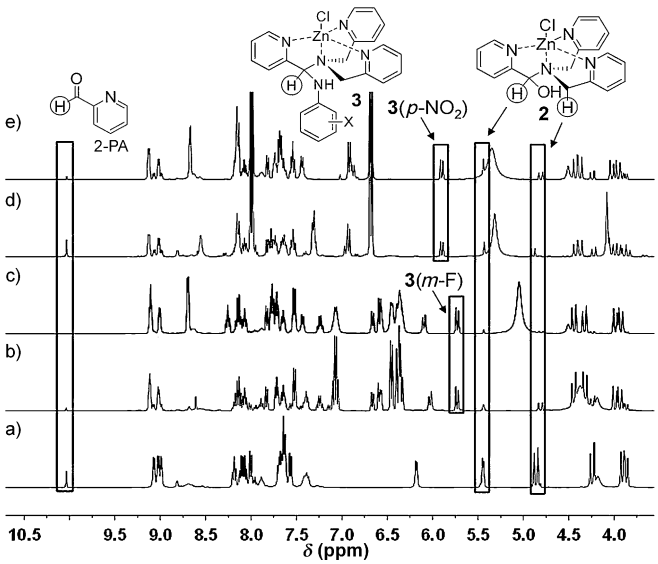

Figure 5. The detection of intermediate **2**. a) The control experiment: The creation of **2** by the assembly of 2-PA and DPA-Zn^{II}; b) and c) The assembly with 3-fluoroaniline in the absence and presence of pyridinium triflate after 1.5 h; d) and e) The assembly with 4-nitroaniline in the absence and presence of pyridinium triflate after 1.5 h.

3 increased (the Supporting Information, Figure S14). In addition, the percentage of imine **1** gradually increased while the peaks for aminal **7** appeared. We rationalize these results as following: 1) Due to the relatively low nucleophility of 4-nitroaniline, its addition to 2-PA is slow and rivaled by DPA; 2) Once the imine **1** forms, however, it rapidly reaches equilibrium with aminals **3** and **7** as a result of its high reactivity; 3) Hemiaminal **2** also slowly transforms to **3**. Thus, in summary, electron-donating groups on the aromatic amine direct the assembly primarily through an imine, albeit with lower equilibrium constants for full assembly. Electron-withdrawing groups on the aromatic amine seem to access both mechanistic pathways (imine and iminium) and give overall more assembly.

The reaction pathways were also confirmed by the multicomponent assembly reaction in the absence of molecular sieves. With *p*-OCH_3, *m*-F, and *p*-NO_2-substituted amines, hemiaminal **2** was observed in all cases, although its amount increases as the arene becomes more electron-deficient (the Supporting Information, Figure S16). This is reasonable because without molecular sieves assisting imine formation the direct DPA addition to 2-PA is more involved. Hence, we have a dynamic multicomponent assembly whose pathway can be modulated by substitution, Brønsted acid, or the addition of molecular sieves.

Mass spectral analysis

To further elucidate the assembly mechanism, ESI-MS experiments were performed to characterize potential intermediates. Because of the dynamic nature of these multicomponent assembly reactions and the lability of the components, fragmentation is likely under mass spectral conditions. Nevertheless, their information sheds light on possible intermediates. Complex **3** was observed in the assembly mixture with 4-methoxyaniline (the Supporting information, Figure S18) with an *m/z* of 510.0 [**3**+Cl], but not complex **2**, which is in good agreement with the NMR spectroscopic studies. For 3-fluoroaniline (the Supporting Information, Figure S20), the corresponding **3** (*m/z* = 498.4, [**3**+Cl]) is also the major species, although both hemiaminal **2** (*m/z* = 405.1, [**2**+Cl]) and iminium **5** (*m/z* = 289.8) were detected, indicative of the emergence of the iminium pathway. In the case of 4-nitroaniline-derived assembly (the Supporting Information, Figure S19), complex **3** (*m/z* = 525.0, [**3**+Cl]) was present. However, significant abundance of **2** (*m/z* = 405.1, [**2**+Cl]) and iminium **5** (*m/z* = 289.3) were present. These findings suggest that **5** is a viable intermediate, and are also consistent with the low nucleophilicity of 4-nitroaniline.

Conclusion

Dynamic covalent reactions (DCRs) of aromatic amines to create imines that convert to TPA-like ligands were studied in detail. The multicomponent assembly was conducted as a means of creating imines in situ and controlling the competing pathway. The equilibrium reaction of 2-PA, DPA, zinc triflate, and aromatic primary amines can be modulated by counteranions and substituents. Halogen anions facilitate the assembly by increasing the thermodynamic stability of the zinc complex through coordination on the axial position of the metal center. The stability of the assembly was further optimized through substituent effects and correlated by a linear free energy relationship (LFER) with σ^+ values. Electron-donating groups, such as *p*-OCH_3, stabilize the imine through quinoidal resonance interactions, whereas electron-withdrawing groups, such as *p*-NO_2 and *p*-CN, destabilize the imine and increase its reactivity. Moreover, the reversibility of the assembly is validated by dynamic component exchange, and the mechanism is elucidated by kinetics and mass spectral analysis. The competing iminium pathway is more pronounced for aromatic amines bearing an electron-withdrawing group. The equilibrium and mechanism insights revealed here should be beneficial to other DCRs involving carbonyl derivatives.

Experimental Section

All assembly reactions were performed in situ in acetonitrile without isolation and purification. Activated 3 Å molecular sieves (4 to 8 mesh), di-(2-picolyl)amine (DPA, 1.2 equiv), primary aromatic amine (3.0 equiv), and tetrabutylammonium salts (1.0 equiv) were added to a stirred solution of pyridine-2-carboxyaldehyde (2-PA, 50–55 mM, 1 equiv) and zinc triflate ([$Zn(OTf)_2$], 1.0 equiv) in [D_3]acetonitrile (0.6 mL). The mixture was stirred at room temperature overnight. The assembly solution was characterized by ^{1}H NMR spectroscopy and ESI-MS.

Acknowledgements

L.Y. thanks The Recruitment Program of Global Youth Experts and Natural Science Foundation of Fujian Province, China

(2014J05024) for support. E.V.A. acknowledges financial support from the National Science Foundation (CHE-1212971).

Keywords: imines · ligands · molecular recognition · self-assembly · substituent effects · zinc

[1] a) S. J. Rowan, S. J. Cantrill, G. R. L. Cousins, J. K. M. Sanders, J. F. Stoddart, *Angew. Chem. Int. Ed.* **2002**, *41*, 898 – 952; *Angew. Chem.* **2002**, *114*, 938 – 993; b) J.-M. Lehn, *Chem. Soc. Rev.* **2007**, *36*, 151 – 160.

[2] a) P. T. Corbett, J. Leclaire, L. Vial, K. R. West, J.-L. Wietor, J. K. Sanders, S. Otto, *Chem. Rev.* **2006**, *106*, 3652 – 3711; b) E. Moulin, G. Cormos, N. Giuseppone, *Chem. Soc. Rev.* **2012**, *41*, 1031 – 1049; c) A. Herrmann, *Chem. Soc. Rev.* **2014**, *43*, 1899 – 1933.

[3] a) J.-M. Lehn, *Science* **2002**, *295*, 2400 – 2403; b) N. Giuseppone, *Acc. Chem. Res.* **2012**, *45*, 2178 – 2188; c) F. Dumitru, Y.-M. Legrand, E. Petit, A. van der Lee, M. Barboiu, *Dalton Trans.* **2012**, *41*, 11860 – 11865; d) K. Kobayashi, M. Yamanaka, *Chem. Soc. Rev.* **2015**, *44*, 449 – 466; e) G. Zhang, M. Mastalerz, *Chem. Soc. Rev.* **2014**, *43*, 1934 – 1947; f) Y. Jin, Q. Wang, P. Taynton, W. Zhang, *Acc. Chem. Res.* **2014**, *47*, 1575 – 1586.

[4] a) V. T. Bhat, A. M. Caniard, T. Luksch, R. Brenk, D. J. Campopiano, M. F. Greaney, *Nat. Chem.* **2010**, *2*, 490 – 497; b) I. M. Serafimova, M. A. Pufall, S. Krishnan, K. Duda, M. S. Cohen, R. L. Maglathlin, J. M. McFarland, R. M. Miller, M. Frödin, J. Taunton, *Nat. Chem. Biol.* **2012**, *8*, 471 – 476; c) S. Ulrich, P. Dumy, *Chem. Commun.* **2014**, *50*, 5810 – 5825; d) I. K. H. Leung, T. Brown Jr, C. J. Schofield, T. D. W. Claridge, *MedChemComm* **2011**, *2*, 390 – 395.

[5] a) M. E. Belowich, J. F. Stoddart, *Chem. Soc. Rev.* **2012**, *41*, 2003 – 2024; b) P. Kovaříček, J.-M. Lehn, *J. Am. Chem. Soc.* **2012**, *134*, 9446 – 9455; c) M. d. Capela, N. J. Mosey, L. Xing, R. Wang, A. Petitjean, *Chem. Eur. J.* **2011**, *17*, 4598 – 4612; d) N. Wilhelms, S. Kulchat, J.-M. Lehn, *Helv. Chim. Acta* **2012**, *95*, 2635 – 2651; e) G. Wang, G. Wu, Z. Wang, X. Zhang, *Langmuir* **2014**, *30*, 1531 – 1535.

[6] a) A. Dirksen, S. Dirksen, T. M. Hackeng, P. E. Dawson, *J. Am. Chem. Soc.* **2006**, *128*, 15602 – 15603; b) J. F. Folmer-Andersen, J.-M. Lehn, *J. Am. Chem. Soc.* **2011**, *133*, 10966 – 10973; c) S. R. Beeren, M. Pittelkow, J. K. M. Sanders, *Chem. Commun.* **2011**, *47*, 7359 – 7361; d) L. A. Tatum, X. Su, I. Aprahamian, *Acc. Chem. Res.* **2014**, *47*, 2141 – 2149.

[7] a) S. P. Black, J. K. M. Sanders, A. R. Stefankiewicz, *Chem. Soc. Rev.* **2014**, *43*, 1861 – 1872; b) Y. Zhang, P. Vongvilai, M. Sakulsombat, A. Fischer, O. Ramström, *Adv. Synth. Catal.* **2014**, *356*, 987 – 992; c) N. Ponnuswamy, F. B. L. Cougnon, J. M. Clough, G. D. Pantoş, J. K. M. Sanders, *Science* **2012**, *338*, 783 – 785; d) A. R. Stefankiewicz, J. K. M. Sanders, *Chem. Commun.* **2013**, *49*, 5820 – 5822; e) K. R. West, K. D. Bake, S. Otto, *Org. Lett.* **2005**, *7*, 2615 – 2618.

[8] a) S. D. Bull, M. G. Davidson, J. M. H. van den Elsen, J. S. Fossey, A. T. A. Jenkins, Y.-B. Jiang, Y. Kubo, F. Marken, K. Sakurai, J. Zhao, T. D. James, *Acc. Chem. Res.* **2013**, *46*, 312 – 326; b) J. Tönnemann, R. Scopelliti, K. O. Zhurov, L. Menin, S. Dehnen, K. Severin, *Chem. Eur. J.* **2012**, *18*, 9939 – 9945; c) R. Nishiyabu, Y. Kubo, T. D. James, J. S. Fossey, *Chem. Commun.* **2011**, *47*, 1124 – 1150.

[9] a) Q. Ji, R. C. Lirag, O. S. Miljanic, *Chem. Soc. Rev.* **2014**, *43*, 1873 – 1884; b) Q. Ji, O. Š. Miljanić, *J. Org. Chem.* **2013**, *78*, 12710 – 12716; c) K. Osowska, O. Š. Miljanić, *J. Am. Chem. Soc.* **2011**, *133*, 724 – 727; d) W. R. Dichtel, O. Š. Miljanić, W. Zhang, J. M. Spruell, K. Patel, I. Aprahamian, J. R. Heath, J. F. Stoddart, *Acc. Chem. Res.* **2008**, *41*, 1750 – 1761.

[10] a) A. Star, I. Goldberg, B. Fuchs, *Angew. Chem. Int. Ed.* **2000**, *39*, 2685 – 2689; *Angew. Chem.* **2000**, *112*, 2797 – 2801; b) P. Wipf, S. G. Mahler, K. Okumura, *Org. Lett.* **2005**, *7*, 4483 – 4486; c) C. Saiz, P. Wipf, E. Manta, G. Mahler, *Org. Lett.* **2009**, *11*, 3170 – 3173; d) B. Buchs née Levrand, G. Godin, A. Trachsel, J.-Y. de Saint Laumer, J.-M. Lehn, A. Herrmann, *Eur. J. Org. Chem.* **2011**, *2011*, 681 – 695.

[11] a) B. Fuchs, A. Nelson, A. Star, J. F. Stoddart, S. Vidal, *Angew. Chem. Int. Ed.* **2003**, *42*, 4220 – 4224; *Angew. Chem.* **2003**, *115*, 4352 – 4356; b) R. Cacciapaglia, S. Di Stefano, L. Mandolini, *J. Am. Chem. Soc.* **2005**, *127*, 13666 – 13671; c) J. A. Berrocal, R. Cacciapaglia, S. D. Stefano, *Org. Biomol. Chem.* **2011**, *9*, 8190 – 8194.

[12] a) L. You, S. R. Long, V. M. Lynch, E. V. Anslyn, *Chem. Eur. J.* **2011**, *17*, 11017 – 11023; b) L. You, J. S. Berman, E. V. Anslyn, *Nat. Chem.* **2011**, *3*, 943 – 948.

[13] M. Kruppa, B. König, *Chem. Rev.* **2006**, *106*, 3520 – 3560.

[14] a) E. H. Cordes, W. P. Jencks, *J. Am. Chem. Soc.* **1963**, *85*, 2843 – 2848; b) K. Koehler, W. Sandstrom, E. H. Cordes, *J. Am. Chem. Soc.* **1964**, *86*, 2413 – 2419; c) R. L. Reeves, *J. Org. Chem.* **1965**, *30*, 3129 – 3135; d) Y. Ogata, A. Kawasaki, *J. Org. Chem.* **1974**, *39*, 1058 – 1061.

[15] a) H. H. Jaffe, *Chem. Rev.* **1953**, *53*, 191 – 261; b) C. Hansch, A. Leo, R. W. Taft, *Chem. Rev.* **1991**, *91*, 165 – 195; c) H. C. Brown, Y. Okamoto, *J. Am. Chem. Soc.* **1958**, *80*, 4979 – 4987.

[16] a) T. T. Tsou, J. K. Kochi, *J. Am. Chem. Soc.* **1979**, *101*, 6319 – 6332; b) C. Amatore, F. Pfluger, *Organometallics* **1990**, *9*, 2276 – 2282; c) V. P. W. Böhm, W. A. Herrmann, *Chem. Eur. J.* **2001**, *7*, 4191 – 4197; d) J. A. Mueller, M. S. Sigman, *J. Am. Chem. Soc.* **2003**, *125*, 7005 – 7013.

[17] H. H. Jo, R. Edupuganti, L. You, K. N. Dalby, E. V. Anslyn, *Chem. Sci.* **2015**, *6*, 158 – 164.

Received: January 10, 2015
Published online on ■■ ■■, 2015

FULL PAPER

Dynamic Covalent Reactions

Y. Zhou, Y. Yuan, L. You, E. V. Anslyn**

■■ – ■■

Dynamic Aminal-Based TPA Ligands

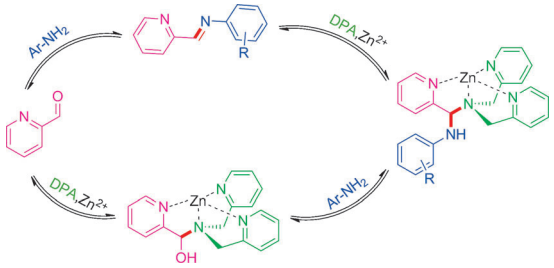

Probing pathways: Dynamic covalent reactions (DCRs) of aromatic amines to create imines that convert to tri(2-picolyl)amine (TPA)-like ligands were studied in detail. The multicomponent assembly was conducted as a means of creating imines in situ and controlling the competing pathway (see figure; DPA = di(2-picolyl)amine).